Resonant Raman scattering in GaAs/AlAs superlattices: The role of electron state mixing

A. Mlayah and R. Carles
Laboratoire de Physique des Solides, Université Paul Sabatier, 118 route de Narbonne, 31062 Toulouse Cédex, France

A. Sayari, R. Chtourou, and F. F. Charfi
Laboratoire de Spectroscopie Moleculaire, Faculté des sciences de Tunis, Campus universitaire, 1060, Tunisia

R. Planel
Laboratoire de Microstructures et de Microélectronique, Centre National de la Recherche Scientifique, Centre National d'Etudes des Télécommunications, Boîte Postal 107, 92225 Bagneux, France

(Received 24 July 1995)

In this work, resonant Raman measurements on a short-period GaAs/AlAs superlattice are presented. Under resonant excitation, near the direct band gap, zone-edge acoustic phonons are observed. Similar scattering has been also recorded in the resonant Raman spectra of an $Al_xGa_{1-x}As$ alloy layer. We show that intervalley electron scattering is at the origin of the observed similarities. This scattering is attributed to the superlattice potential for the GaAs/AlAs superlattice, and to the potential fluctuations for the $Al_xGa_{1-x}As$ alloy. The present analysis gives a clear interpretation of the Raman scattering by zone-edge acoustic phonons in both systems. Moreover, the role of disorder is discussed in terms of an activation of folded acoustic and coupled confined-interface phonons.

I. INTRODUCTION

Raman scattering in semiconductor quantum wells (QW's) and superlattices (SL's) showed that, besides the existence of folded and confined phonon modes, the interface involving at least one polar semiconductor sustains localized optic phonon modes, the so-called interface phonons[1] (IF). The latter have been studied earlier by Fuchs and Kliewer[2] using a dielectric continuum approach for a periodic two-layer system. The possible use of Raman scattering by IF phonons, as a sensitive probe of the interface quality, has given rise to a lot of works on GaAs/AlAs and $GaAs/Al_xGa_{1-x}As$ SL's.[3–6] Indeed, the observation of finite in-plane wave-vector IF phonons in the Raman spectra measured in backscattering geometry, and the strong outgoing resonance reported in several data, are typical of the breakdown of the wave-vector conservation rule, i.e., of disorder effects.[7–10] It has been suggested that the lack of in-plane wave vectors in the three-step resonant Raman process can be balanced by an additional intermediate step during which the photoexcited electron (or hole) is elastically scattered.[11] The elastic scattering arises from electron-charged impurities interaction and/or from interface roughness.

Moreover, disorder effects have led to a complete reinterpretation of Raman scattering in SL's and QW's. Indeed, earlier works attributed the features observed in the GaAs and AlAs optic mode regions either to confined or to interface phonons. Within the hydrodynamic model[1] (HD) the quantized wave vectors q_z along the SL axis are given by

$$q_z=\frac{m\pi}{(n+1)a}, \quad 1\leqslant m\leqslant n, \tag{1}$$

where a is the monolayer width, n the number of monolayers in the confining layer, and m an integer. For odd m, the measured frequencies of the confined LO_m modes map quite well onto the bulk dispersion curves. However, for even m discrepancies are found, which Shields *et al.*[12,13] explained. They showed that most of the resonant Raman scattering (RRS), commonly attributed to even order confined modes, is in fact due to coupled odd confined-interface modes.

Previous assignments assumed vanishing in-plane wave vectors for which the vibrational amplitude and electromagnetic fields are decoupled. Thus, confined and interface modes were treated within independent hydrodynamic and electromagnetic approaches. Moreover, both approaches can be used to determine the symmetry of the Coulomb potential associated with the confined modes, and thus the Raman selection rules for the Fröhlich electron-phonon interaction.[14–16] The obtained results are inconsistent, depending on the approach.[17] In fact, contradictions come out when the coupling between the mechanical and electromagnetic field is ignored. Trallero-Giner and Comas[18] and Guillemot and Clerot[19] used a continuum approach, along the lines of Born and Huang, for the vibrational amplitude field. The coupling to the electromagnetic field was fully taken into account in the equation of motion. Quantization of the coupled electromechanic field was achieved using both mechanical and electromagnetic boundary conditions. The so obtained eigenmodes are hybrid confined-interface modes. Their dispersion exhibits, at finite in-plane wave vectors, gaps due to anticrossing of the interface branches with the odd-order confined modes.[12,13]

These gaps produce, in the resonant Raman spectra, dips of which frequencies coincide with those of the odd-order confined modes. The maxima between these minima occur at frequencies close to those of the even-order confined modes. This new interpretation corrects previous attributions of the maxima to even-order confined modes.

In this paper we report a study of RRS in a short-period GaAs/AlAs SL. Light scattering by the folded acoustic phonons, as well as the coupled confined-interface phonons, is discussed.

First, it is shown that the Raman spectra, recorded with excitation energies close to the direct $\Gamma_v-\Gamma_c$ band gap, exhibit scattering due to bulklike zone-edge acoustic phonons. Zone-edge phonons have been already observed by Hayes *et al.*,[20] as replicas of the photoluminescence line associated with recombinations across the pseudodirect Γ_v-X_z band gap. RRS at the pseudodirect transition, also showed zone-edge phonons.[21,22] In our case, scattering by zone-edge phonons is observed even for resonant excitation at the direct $\Gamma_v-\Gamma_c$ bandgap. Similar scattering has been also recorded in the resonant Raman spectra of $Al_xGa_{1-x}As$ alloys. It is shown that intervalley electron scattering is at the origin of the observed similarities. This scattering is attributed to the superlattice potential[23] for the GaAs/AlAs superlattice, and to the potential fluctuations for the $Al_xGa_{1-x}As$ alloy

Second, we show that the standard hydrodynamic and electromagnetic models fail to explain all the structures we observe in the GaAs optic mode region. A comparison of our data with the recent interpretation, proposed by Shields *et al.*[12,13] is presented. To the best of our knowledge such a comparison has never been performed for very narrow confining layers.

II. EXPERIMENT

The superlattice used in this work was grown by molecular-beam epitaxy on a [100]-oriented GaAs substrate. It consists of 100 periods of 3 and 10 monolayers of GaAs and AlAs, respectively. This superlattice is of type II: The lowest-energy excitation (Γ_v-X_z) is pseudodirect.[24] The direct $\Gamma_v-\Gamma_c$ transition was found at 2.4 eV from photoluminescence measurements. This value is in agreement with band-structure calculations. The bandwidth of the first electronic subband was estimated to be 43 meV.

The Raman measurements were carried out at the liquid nitrogen temperature and in near backscattering geometry. The scattered light was analyzed using a triple spectrometer coupled with a conventional photon counting system. Several lines of an Ar laser have been used for excitation near the direct $\Gamma_v-\Gamma_c$ transition.

III. RESULTS AND DISCUSSION

A. Acoustic mode region

In Fig. 1, Raman spectra recorded from the $(GaAs)_3/(AlAs)_{10}$ SL are shown. The lower spectrum (a) was excited in resonance with the direct $\Gamma_v-\Gamma_c$ transition using the 5145-Å line (2.41 eV). The intense low-frequency doublet, clearly seen in both Stokes and anti-Stokes regions, is due to the folded (first order of folding) longitudinal acoustic (LA) phonons.[25] Following Ref. 26 their frequencies, ω, map onto the dispersion curve of acoustic waves in a medium with a periodic layering of the elastic properties

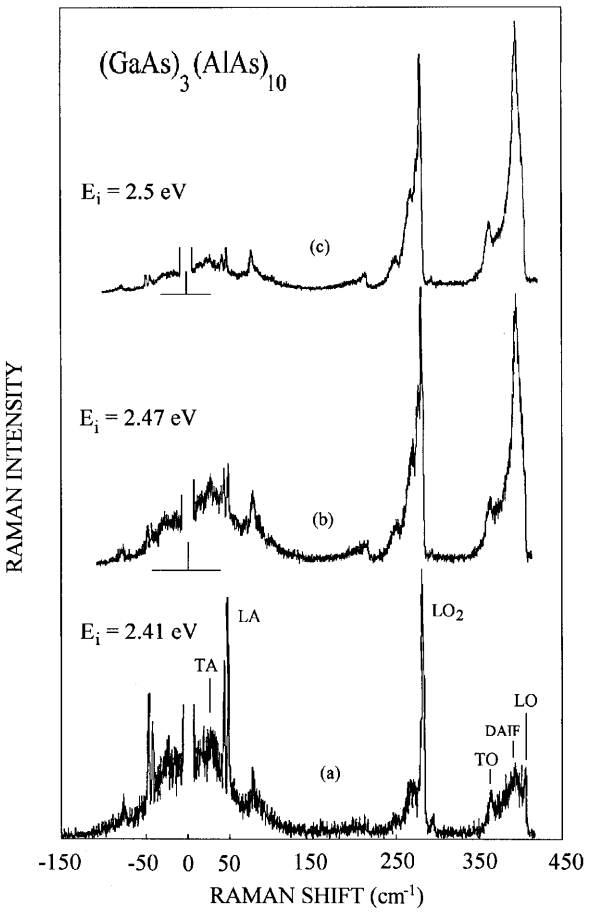

FIG. 1. Raman spectra of the GaAs/AlAs SL, recorded for incoming (spectrum a) and outgoing (spectra b and c) resonance conditions. The structure labeled DAIF refers to disorder activated interface phonons.

$$\cos(qd)=\cos\left(\frac{\omega d_1}{\nu_{1,l(t)}}\right)\cos\left(\frac{\omega d_2}{\nu_{2,l(t)}}\right)-\frac{1+h^2}{2h}\sin\left(\frac{\omega d_1}{\nu_{1,l(t)}}\right)\sin\left(\frac{\omega d_2}{\nu_{2,l(t)}}\right), \qquad (2)$$

where, $h=\rho_1\nu_1/\rho_2\nu_2$, $d=d_1+d_2$ and ρ_1, ρ_2, $\nu_{1,l(t)}$, $\nu_{2,l(t)}$, d_1, d_2 are the densities, longitudinal (transverse) sound velocities and thicknesses of the two materials: Ref. 27 gives $\rho_1=5.36$ g cm^{-3}, $\nu_{l1}=4.707\times10^5$ cm s^{-1}, $\nu_{t1}=3.329\times10^5$ cm s^{-1} for GaAs, and $\rho_2=5.36$ g cm^{-3}, $\nu_{l2}=5.654\times10^5$ cm s^{-1}, $\nu_{t2}=3.957\times10^5$ cm s^{-1} for AlAs. In backscattering geometry the phonon wave vector q along the superlattice axis equals $4\pi n/\lambda_i$; where n is the refractive index. For $\lambda_i=5145$ Å, one gets $q=9.10^5$ cm^{-1}.

From Eq. (2) and the measured frequencies (43.4 and 48 cm^{-1}) of the LA doublet, we have deduced $d_1=10$ Å and $d_2=29$ Å. Using these values as inputs in Eq. (2) we have estimated the frequencies of the folded (first order of folding) TA phonons to be 30.3 and 34.2 cm^{-1}. The former value is roughly comparable to the frequency (28 cm^{-1}) of the weak scattering shown in Fig. 1. This discrepancy is mainly due to the sublinear dispersion of TA phonons around the wave vector π/d. As a matter of fact, selection rules prohibit back-

scattering of light by folded acoustic TA phonons for [100]-oriented superlattices.[1] The observation of such modes in our measurements is due to disorder effects that we discuss in the following.

From Fig. 1, one notes that the folded acoustic phonons are superimposed over a continuum of acoustic modes (5–50 cm^{-1}). This suggests that not only superperiodicity but also thickness fluctuations of the layers have to be taken into account. Indeed, spatial fluctuations of the potentials experienced by the electrons and atoms originate in complex momenta for the electronic and vibronic excitations, which so become localized in real space. As a consequence, the electron as well as the phonon states are distributed in the reciprocal space, and the energy levels are inhomogeneously broadened. This also means that the conservation law is partially violated during light scattering: The scattering, at a given frequency, can no more be ascribed to a well-defined phonon mode. It is rather due to a distribution of modes. Their contribution to light scattering leads to the broad band observed in Fig. 1. So, this band should reflect the partially activated one-dimensional density of states of folded (LA and TA) acoustic phonons.

The spectra *b* and *c*, shown in Fig. 1, were excited using the 5017-Å (2.47 eV) and 4965-Å (2.5 eV) laser lines. The weak structures observed at 78 and 214 cm^{-1} in spectrum *a* clearly come out in spectra *b* and *c*. For more details, Fig. 2 shows an extension, into the acoustic mode region, of the spectrum (*d*) recorded with the 4880-Å (2.54 eV) laser line. This figure includes, for comparison the spectra (*e* and *f*) of an $Al_{0.75}Ga_{0.25}As$ layer of which composition equals the average composition (d_2/d) of the superlattice. The band gap of this alloy is indirect, and the ordering of the conduction-band minima is Γ, L, X.[28] Spectra *f* and *e* were recorded out of resonance and close to resonance (2.62 eV) with the direct ($\Gamma_v-\Gamma_c$) band gap, respectively. Under resonant excitation, new peaks develop and are ascribed to TA and LA acoustic modes. Moreover, scattering due to substractive combinations of GaAs-like and AlAs-like optic (LO and TO) modes is observed. The assignments of the acoustic modes, reported in Fig. 2, are based on the density-of-states singularities at the X or L points of the end-parent crystals (GaAs and AlAs).[29,30] The scattering by zone-edge acoustic phonons shows evidence of phonon-assisted intervalley electron transfer ($\Gamma-X$ and $\Gamma-L$). The observation of such modes is allowed owing to the breakdown of the wave-vector conservation law, induced by the alloy disorder. The similarities between the alloy and SL spectra suggest that the structures located at 78 and 214 cm^{-1} (spectrum *d*) are bulklike TA and LA modes derived from the X point of the Brillouin zone (BZ). Note that bulklike LA(L) modes are not observed in the SL spectrum (Fig. 2, spectrum *d*).

By using RRS at the pseudodirect Γ_v-X_z band gap, of small period GaAs/AlAs SL's Hayes *et al.*[20] and Tribe *et al.*[21,22] have observed bulklike LA(X) modes. The normally forbidden resonance at the pseudodirect band gap has been attributed to the mixing between Γ_c and X_z states. We would like to stress that in our Raman measurements zone-edge acoustic phonons are also observed at the direct $\Gamma_v-\Gamma_c$ SL band gap. Moreover, our photoluminescence measurements showed electron recombinations across the pseudodirect Γ_v-X_z gap, and thus the existence of Γ_c-X_z state mixing. We attribute the observation of scattering by zone-edge acoustic phonons to the fact that the conduction electron states are indeed mixed Γ_c-X_z states.

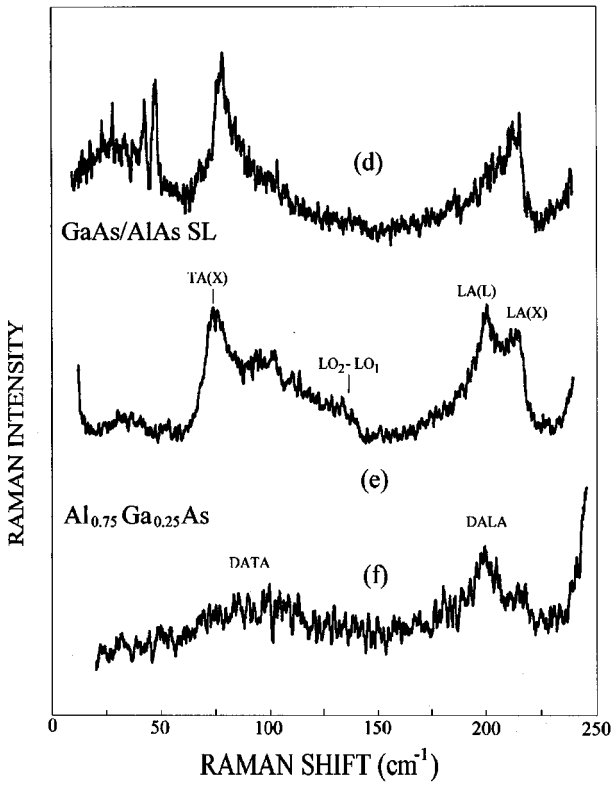

FIG. 2. Comparison of the low-frequency Raman spectra of the GaAs/AlAs SL (spectrum *d*) and the $Al_{0.75}Ga_{0.25}As$ alloy (spectra *e* and *f*). Spectrum *f* was recorded out of resonance and spectrum *e* close to the direct transition of the alloy. The bands labeled DATA and DALA refer to disorder-activated transverse and longitudinal acoustic modes, respectively. The subscripts 1 and 2 refer to the GaAs-like and AlAs-like optic bands, respectively.

The Γ_c-X_z mixing arises from the BZ folding, which allows states, originating in the Γ_c and X_z valleys, to occur at the same wave vector (in the folded BZ). These states mix due to nonorthogonality of the wave functions at the Γ_c and X_z points.[31,32] Following Morrison, Brown, and Jaros,[33] the mixing can be described as a coupling of these wave functions via the potential modulation (ΔV) along the SL axis. Let us define the dimensionless parameter $\eta=\Delta V_{\Gamma_c,X_z}/\Delta E_{\Gamma_c,X_z}$, where $\Delta V_{\Gamma_c,X_z}=\langle X_z|\Delta V|\Gamma_c\rangle$ is the matrix element between the SL Γ_c and X_z states, and $\Delta E_{\Gamma_c,X_z}=E_{\Gamma_c}-E_{X_z}$, the energy separation between these states. Then, for $\eta\ll 1$ (weak-coupling regime), the coupled $\Gamma_{c\text{-like}}$ state can be written as follows

$$|\Gamma_{c\text{-like}}\rangle=\frac{1}{\sqrt{1+|\eta|^2}}\,|\Gamma_c\rangle+\frac{\eta}{\sqrt{1+|\eta|^2}}\,|X_z\rangle. \qquad (3)$$

The Raman intensity corresponding to phonon-mediated electron scattering between $|\Gamma_{c\text{-like}}\rangle$ and $|\Gamma'_{c\text{-like}}\rangle$ conduction-band states is determined by the scattering amplitude

$$\frac{\langle\Gamma_v|H_{pt}|\Gamma'_{c\text{-like}}\rangle\langle\Gamma'_{c\text{-like}}|H_{pn}|\Gamma_{c\text{-like}}\rangle\langle\Gamma_{c\text{-like}}|H_{pt}|\Gamma_v\rangle}{[E_s-E_{\Gamma'_{c\text{-like}}}][E_i-E_{\Gamma_{c\text{-like}}}]}, \quad (4)$$

where H_{pt} and H_{pn} are the Hamiltonians describing electron-photon and electron-phonon interactions. The difference $E_{\Gamma'_{c\text{-like}}}-E_{\Gamma_{c\text{-like}}}$ between the energies associated with the $|\Gamma_{c\text{-like}}\rangle$ and $|\Gamma'_{c\text{-like}}\rangle$ states is the energy, $\hbar\omega_{pn}$ of the emitted phonon. E_i and E_s are the energies of the incident and scattered photons, respectively. Since the $|\Gamma_{c\text{-like}}\rangle$ and $|\Gamma'_{c\text{-like}}\rangle$ states are linear combinations of $|\Gamma_c\rangle$ and $|X_z\rangle$ states, the matrix element $\langle\Gamma'_{c\text{-like}}|H_{pn}|\Gamma_{c\text{-like}}\rangle$ includes phonon-induced intravalley ($\Gamma_c-\Gamma_c, X_z-X_z$) and intervalley ($\Gamma_c-X_z$) scattering. Momentum conservation during this latter process implies that, in the $\Gamma-X_z$ direction, only zone-edge phonons at the X point can be involved. Following the recent work of Raichev,[34] who calculated electron scattering rates in short-period GaAs/AlAs SL, both TA and LA modes contribute to the phonon-mediated Γ_c-X_z transfer. This well accounts for our data of Fig. 1 and Fig. 2 (spectrum d). It is worthwhile to note that in the three-step resonant Raman process, here proposed [Eq. (4)], the emission of zone-edge phonon modes is allowed. Hence, no additional elastic scattering step is required to account for the observation of zone-edge phonon modes in the first-order Raman spectra. In fact, this step is useless due to the Γ_c-X_z mixing induced by the superlattice potential. Indeed, using Eq. (3) one can isolate from the matrix element $\langle\Gamma'_{c\text{-like}}|H_{pn}|\Gamma_{c\text{-like}}\rangle$ the scattering path responsible for the emission of zone-edge phonon modes. For $|\eta|^2\ll 1$, one gets

$$\frac{\langle\Gamma'_c|\Delta V|X_z\rangle\langle X_z|H_{pn}|\Gamma_c\rangle}{(E_{\Gamma_c}-\hbar\omega_{pn}-E_{X_z})}. \quad (5)$$

Since ΔV is a static spatial modulation of potential, the matrix element $\langle\Gamma'_c|\Delta V|X_z\rangle$ is associated with the elastic scattering of an electron from the X_z state to the Γ'_c state. Owing to the superperiodicity, the potential modulation ΔV can be developed over plane waves with wave vectors $G=2m\pi/d$. Momentum conservation imposes that only the $G=\pi/a$ component can couple X_z and Γ_c states. In a similar way, only phonon modes arising from the highest order of folding ($G=\pi/a$) can give nonvanishing $\langle X_z|H_{pn}|\Gamma_c\rangle$ matrix element. This is the reason why the acoustic phonon modes observed in spectrum d originate from the X point of the BZ.

Moreover, neglecting the small difference in energy between the $|\Gamma_c\rangle$ and $|\Gamma_{c\text{-like}}\rangle$ states, Eq. (4) shows that an incoming resonance is expected at the $\Gamma_v-\Gamma_c$ transition. Overlapping of incoming and outgoing resonances is also expected, due to the small energies of acoustic phonons (10 and 26 meV for TA and LA phonons, respectively). In addition, the elastic scattering step is automatically resonant. This leads to a triply resonant process that compensate the rather weak Γ_c-X_z mixing ($\eta\ll 1$).

From the foregoing discussion it emerges that intervalley electron scattering, mediated by zone-edge phonons, is a common mechanism for indirect band gap GaAs/AlAs SL and $Al_xGa_{1-x}As$ alloys. This is at the origin of the similarities observed between the spectra of Fig. 2. However, for the GaAs/AlAs SL, emission of zone-edge phonons is allowed and no breakdown of the wave-vector conservation law has to be invoked. The apparently missing wave vector, in the Raman scattering process, is provided by the SL potential (Γ_c-X_z mixing). For the $Al_xGa_{1-x}As$ system, emission of zone-edge phonons is observed thanks to the alloy disorder. In this case the breakdown of the wave-vector conservation law can be accounted for by adding an additional intermediate step during which the electron is elastically scattered back from a zone-edge valley to the Γ_c point. The elastic scattering is due to random potential fluctuations. The wave-vector selectivity disappears, and X or L valleys can be involved (Fig. 2, spectrum e).

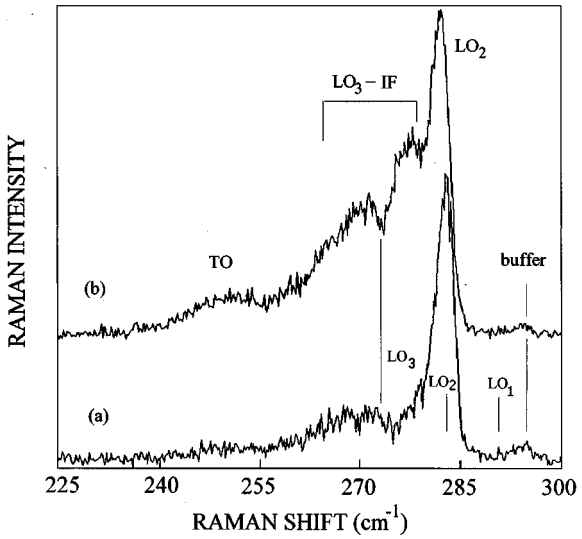

FIG. 3. Extension of spectra a and b of Fig. 1, into the GaAs optic mode region. The vertical lines show the frequencies of the confined LO modes, calculated using the hydrodynamic model. The LO peak originating in the GaAs buffer layer is also shown. The weak scattering lying around 248 cm^{-1} is due to confined TO modes.

B. Optic mode region

The outgoing photons giving rise to the optic bands of GaAs in Fig. 1, spectrum b and of AlAs in Fig. 1, spectrum c, are in resonance with the upper edge energy (2.443 eV) of the $\Gamma_v-\Gamma_c$ transition. The energy difference between the GaAs and AlAs vibrational modes explains the reversal of the GaAs/AlAs intensity ratio from b to c. Figure 3, spectra a and b show an extension of spectra a and b of Fig. 1 into the GaAs optical range. Since the GaAs layer contains three monolayers, only three confined LO_m modes, $m=1$, 2, and 3, are expected [Eq. (1)]. The vertical lines shown in Fig. 3 indicate the corresponding frequencies calculated using Eq. (1) and the GaAs LO phonon dispersion curve.

For incoming resonance (spectrum a), only the LO_2 mode is observed. This is consistent with the hydrodynamic model: The Coulomb potential associated with even-order confined modes is symmetric with respect to the center of the confining layer, whereas that of odd-order confined modes is antisymmetric.[35] Thus, when considering intrasubband electron transitions, the Fröhlich electron-phonon interaction, which dominates at resonance, implies even-order confined modes (only LO_2 mode in our case). Odd-order confined

modes are seen out of resonance since in this case the deformation-potential mechanism dominates.[35]

The weak scattering lying around 270 cm^{-1} (in spectrum *a*) strongly comes out and a new structure emerges at 277 cm^{-1} for outgoing resonance conditions (spectrum *b*). None of these features can be assigned to even-order confined modes, since the GaAs layer cannot sustain additional even modes besides the LO_2. This shows the limitation of the hydrodynamic approach.

On the other hand, the electromagnetic model predicts interface phonon bands within the LO-TO ranges of GaAs and AlAs. The participation of these modes is strictly forbidden in backscattering geometry.[35] Nevertheless, thickness fluctuations of the layers and interface roughness break down the wave-vector conservation law, and thus allow scattering by interface modes at finite in-plane wave vectors. This results in a broad band located between the LO and TO frequencies,[3–6] but cannot account for both of the structures observed in spectrum *b*.

In fact, only the coupled hydrodynamic-electromagnetic approach[12,13] gives a clear understanding of spectrum *b*: The structures at 270 and 277 cm^{-1} arise from a unique band with a dip at 273 cm^{-1}. This disorder-activated band reflects the two-dimensional density of mixed LO_3-interface phonon states. The dip is associated with the gap due to anticrossing of the interface branch with the LO_3 confined mode. The in-plane dispersion of the LO_3 mode is rather weak in comparison with the interface branch. Hence, the anticrossing occurs close to the LO_3 mode frequency, which can be deduced from the HD model. This is in good agreement with our data (Fig. 3, spectrum *b*): The dip in the scattered intensity coincides with the frequency of the LO_3 confined mode, which has been calculated using Eq. (1) and the bulk LO dispersion curve.

In the AlAs optic mode region (Fig. 1), the scattering lying between the LO and TO signals is also due to disorder-activated IF phonon modes (DAIF). No gap is observed because of the rather weak dispersion of the AlAs LO modes: The IF phonon branch anticrosses with the odd-order confined modes close to the LO mode frequency.

The spectra of Fig. 3 show that the LO_3-IF feature comes out more strongly for outgoing (spectrum *b*) than incoming (spectrum *a*) resonance. It has been suggested[12,13] that for outgoing resonance, Raman scattering occurs via a four-step process. The additional step accounts for the observation of phonon modes with large wave vectors. In this step the photocreated electron (or hole) is elastically scattered to finite wave-vector states associated with the in-plane motion. It is then inelastically scattered back by phonons via Fröhlich interaction. The elastic scattering originates in the potential fluctuations due to interface roughness. On one hand, this process should lead to enhancement of the scattered intensity, providing that the phonon dispersion does not change rapidly. On the other hand, the elastic scattering step is suppressed for incoming resonance due to the lack of states to scatter to. Hence, outgoing resonance is expected to be stronger than incoming for both GaAs and AlAs optic bands, as observed in the spectra of Figs. 1 and 3.

IV. CONCLUSION

In summary, we have pointed out the origin of the strong similarities between resonant Raman spectra of GaAs/AlAs SL and $Al_xGa_{1-x}As$ alloys. We have shown that, for both of these systems, the Raman processes involving zone-edge acoustic phonons are due to intervalley electron scattering. In the case of the GaAs/AlAs SL, the static potential modulation along the superlattice axis mixes the Γ_c and X_z states, and this results in an allowed triply resonant Raman process involving TA(X) and LA(X) phonons. For the $Al_xGa_{1-x}As$ solid solutions, intervalley electron scattering occurs because of the random potential fluctuations associated with the alloy disorder. For the GaAs/AlAs SL, disorder effects have been discussed in terms of breakdown of the wave-vector conservation law, which permits scattering by phonons at finite in-plane wave vectors. The activation of such modes accounts well for the shape of the optical bands in superlattices. The present analysis is in perfect agreement with the recent model proposed by Shields *et al.*[12,13]

[1] B. Jusserand and M. Cardona, in *Light Scattering in Solids V*, Topics in Applied Physics Vol. 66 (Springer, Berlin, 1989).

[2] R. Fuchs and K. L. Kliewer, Phys. Rev. **140**, A2076 (1965).

[3] A. K. Sood, J. Menendez, M. Cardona, and K. Ploog, Phys. Rev. Lett. **54**, 2115 (1985).

[4] Ph. Lambin, J. P. Vigneron, A. A. Lucas, P. A. Thiry, M. Liehr, J. J. Pireaux, and R. Caudano, Phys. Rev. Lett. **56**, 1842 (1986).

[5] A. K. Arora, A. K. Ramdas, M. R. Melloch, and N. Otsuka, Phys. Rev. B **36**, 1021 (1987).

[6] M. P. Chamberlain, M. Cardona, and B. K. Ridley, Phys. Rev. B **48**, 14 336 (1993).

[7] H. D. Fuchs, D. J. Mowbray, M. Cardona, S. A. Chalmers, and A. C. Gossard, Solid State Commun. **79**, 223 (1991).

[8] D. Gammon, R. Merlin, and H. Morkoç, Phys. Rev. B **35**, 2552 (1987).

[9] G. Ambrazevicius, M. Cardona, R. Merlin, and K. Ploog, Solid State Commun. **65**, 1035 (1988).

[10] D. N. Mirlin, A. A. Sirenko, and R. Planel, Solid State Commun. **91**, 545 (1994).

[11] T. A. Gant, N. Delaney, M. V. Klein, R. Houdre, and H. Morkoç, Phys. Rev. B **39**, 1696 (1989).

[12] A. J. Shields, M. Cardona, and K. Eberl, Phys. Rev. Lett. **72**, 412 (1994).

[13] A. J. Shields, M. P. Chamberlain, M. Cardona, and K. Eberl, Phys. Rev. B **51**, 17 728 (1995).

[14] N. Mori and T. Ando, Phys. Rev. B **40**, 6175 (1989).

[15] J. J. Licari and Roger Evard, Phys. Rev. B **15**, 2254 (1977).

[16] K. Huang and B. Zhu, Phys. Rev. B **38**, 13 377 (1988).

[17] B. K. Ridley and M. Babiker, Phys. Rev. B **43**, 9096 (1991).

[18] C. Trallero-Giner and F. Comas, Phys. Rev. B **37**, 4583 (1988).

[19] C. Guillemot and F. Clerot, Superlatt. Microstruct. **8**, 263 (1990).

[20] W. Hayes, R. Springett, M. S. Skolnick, G. W. Smith, and C. R. Whitehouse, Semicond. Sci. Technol. **7**, 379 (1992).

[21] W. R. Tribe, P. C. Klipstein, R. A. Wodey, and J. S. Roberets, Phys. Rev. B **51**, 9735 (1995).

[22] W. R. Tribe, S. G. Lyapin, P. C. Klipstein, G. W. Smith, and R. Grey, Superlatt. Microstruct. **15**, 293 (1994).
[23] J. B. Xia and Y. C. Chang, Phys. Rev. B **42**, 1781 (1990).
[24] D. Scalbert, J. Cernogora, M. Maaref, F. F. Charfi, and R. Planel, Solid State Commun. **70**, 945 (1989).
[25] C. Colvard, R. Merlin, M. V. Klein, and A. C. Gossard, Phys. Rev. Lett. **45**, 298 (1980).
[26] S. M. Rytov, Akust. Zh. **2**, 71 (1956) [Sov. Phys. Acoust. **2**, 68 (1956)].
[27] S. Adachi, J. Appl. Phys. **58**, R1 (1985).
[28] A. K. Saxena, J. Phys. C **13**, 4323 (1980).
[29] R. Carles, N. Saint-Cricq, A. Zwick, M. A. Renucci, and J. B. Renucci, Nuovo Cimento **2D**, 1712 (1983).
[30] A. Kobayashi, John D. Dow, and Eoin P. O'Reilly, Superlatt. Microstruct. **1**, 471 (1985).
[31] M. Maaref, F. F. Charfi, D. Scalbert, C. Benoit à la Guillaume, and R. Planel, Phys. Status Solidi B **170**, 637 (1992).
[32] M. S. Kolnick, G. W. Smith, I. L. Spain, C. R. Whitehouse, D. C. Herbert, D. M. Whittaker, and L. J. Reed, Phys. Rev. B **39**, 11 191 (1989).
[33] I. Morrison, L. D. L. Brown, and M. Jaros, Phys. Rev. B **42**, 11 818 (1990).
[34] O. E. Raichev, Phys. Rev. B **49**, 5448 (1994).
[35] A. K. Sood, J. Menendez, M. Cardona, and K. Ploog, Phys. Rev. Lett. **54**, 2111 (1985).